Single- and Double-Wall Cylinder Noise Reduction

F. J. Balena,* R. A. Prydz,† and J. D. Revell‡
Lockheed-California Company, Burbank, California

The noise reductions of three small cylinders covering a range of stiffness were measured in a reverberant field environment. A leaded-vinyl septum was used for an inner wall in double-wall configuration studies. The measured noise reduction data are compared with predicted noise reductions. The prediction method is shown to be accurate for the unstiffened and moderately stiffened cylinders and less accurate for highly stiffened cylinders. An acoustical loss factor is introduced to improve the agreement between theory and experiment for the double-wall configurations. The cylinder noise reduction measurements are believed to be the first published test results for double-wall cylinders and they have important application to the study of high-speed turboprop (propfan) interior noise control.

Introduction

AIRCRAFT interior noise control is an important consideration for crew performance and passenger comfort. As new commercial aircraft, especially turboprop aircraft, are brought into the marketplace, a considerable effort will be put forth to insure acceptably quiet interiors. New fuel efficient aircraft will eventually replace the older, less efficient aircraft in service today and aircraft replacements will accelerate as the cost of fuel continues its upward spiral. The aircraft propulsion system with the highest efficiency is the turboprop: thus, significant interest is developing for advanced high-cruise-speed propeller aircraft. NASA is now completing the initial phase of a program to develop the technology base for an advanced turboprop propulsion system, using an advanced, highly swept, multibladed propeller concept called "propfan."[1]

The studies described in Refs. 1-3 indicate that a double-wall fuselage design (utilizing a heavy trim panel separated from the outer fuselage by an air gap and a fiberglass blanket) provides a highly efficient treatment for reducing the transmission of propeller noise to the interior of a propfan aircraft. Because propfan noise is characterized by unusually high blade passage frequencies such designs are especially appropriate. The work described here represents a preliminary effort to evaluate the efficiency of double-wall noise reduction designs, since at present there are no published data on double-wall cylinder noise reduction. The noise reductions of three small-diameter cylinders were tested at the Lockheed Rye Canyon Acoustics Laboratory and compared with predictions of Refs. 1 and 2. The small-cylinder tests and theoretical development work were performed during Lockheed-funded independent research programs. Additional NASA contract work is in progress to provide laboratory verification of the analytical prediction method for a commuter-aircraft-sized fuselage.[4] Additional in-house research and development work is in progress to improve and refine the prediction method. The objectives of the Lockheed research and development effort are:

1) Establishment of a data base of reliable noise reduction data for both double- and single-wall cylinders.

2) Evaluation of the current prediction method by comparison with the measured data base.

Presented as Paper 81-1968 at the AIAA 7th Aeroacoustics Conference, Palo Alto, Calif., Oct. 5-7, 1981; submitted Oct. 13, 1981; revision received July 26, 1982.

*Research and Development Engineer, Acoustics Department.
†Research and Development Scientist, Acoustics Laboratory.
‡Research and Development Scientist, Acoustics Department. Associate Fellow AIAA.

Experimental Investigation

Test Cylinders

Figure 1 shows a sketch of the three cylinders that were used for the noise reduction studies. Each of the cylinders is a riveted open-ended aluminum structure. The unstiffened cylinder (I) is 78 in. long and 20 in. in diameter with a skin thickness of 0.032 in. The ring-stiffened cylinder (II) is also 78 in. long but has a diameter of 24 in. and a 0.025 in. skin thickness. Ring spacing is 18 in. The third cylinder (III) is stiffened with both ring frames and stringers. It also has a length of 78 in. and a diameter of 24 in. Skin thickness is 0.032 in. and ring spacing is 8.25 in. and stringer spacing is 4.0 in. Construction of cylinder III was facilitated by attaching the rings to the outer surface of the skin and the stringers to the inner surface. Table 1 summarizes the structural dimensions and properties of the three test cylinders.

Test Configurations

Noise reduction tests were performed for each of the three cylinders with and without a limp leaded-vinyl inner wall. A lightweight skeletal structure was used to support the inner wall. A sketch of the double-wall configuration is shown in Fig. 2. End closures with high transmission loss were used to minimize noise transmission through the ends of each cylinder. Since the prediction method assumes that the interior volume is totally absorptive, two cylindrical centerbodies of acoustical foam were fabricated, one for the 20 in. cylinder and one for the 24 in. cylinders. The relatively large and highly absorptive centerbodies were used to minimize the formation of standing wave acoustic modes inside the test cylinder. This not only simulated the Koval/Smith analytical assumption but also provided for the direct measurement of sound transmission loss.

Instrumentation and Test Procedures

The noise reductions of three aluminum cylinders were measured in a $13 \times 25 \times 20$ ft high reverberant chamber. The test specimen was positioned 4 ft above the reverberant chamber floor with the axis of the cylinder parallel to the floor. Changing the orientation of the cylinder had no measurable effect on the noise levels measured inside the cylinder. A single microphone on a rotating boom was used to measure the noise inside the test chamber. Three microphones were located inside the cylinder to measure the transmitted noise. The three interior microphones were flush mounted in the absorbent centerbody, one centrally located in the axial direction and the other two 18 in. fore and aft of the central microphone. Averages of the three flush-mounted

Table 1 Test configurations

Configuration No.	Cylinder	Surface density, psf Outer wall	Surface density, psf Inner wall	Total wall density, psf	Wall depth, in.
1	I	0.46	–	0.46	–
2	I	0.46	0.28	0.74	1.0
3	II	0.39	–	0.39	–
4	II	0.39	0.28	0.67	1.5
5	III	1.08	–	1.08	–
6	III	1.08	0.28	1.36	1.5

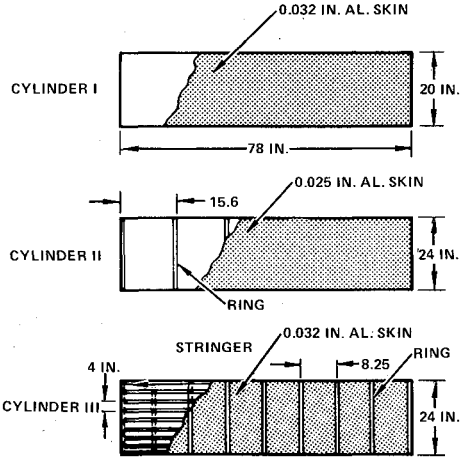

Fig. 1 Test cylinders.

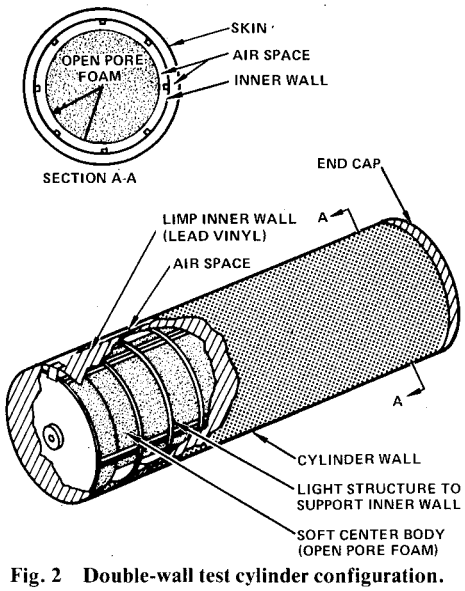

Fig. 2 Double-wall test cylinder configuration.

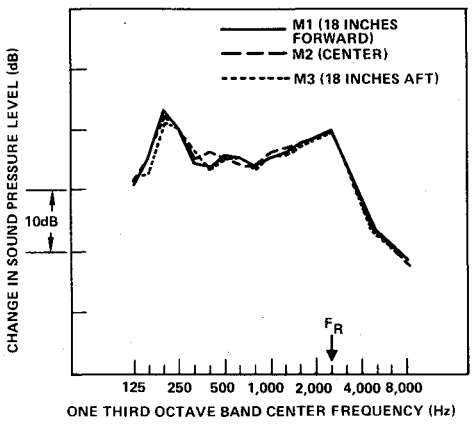

Fig. 3 Cylinder II interior noise spectra for a single-wall configuration.

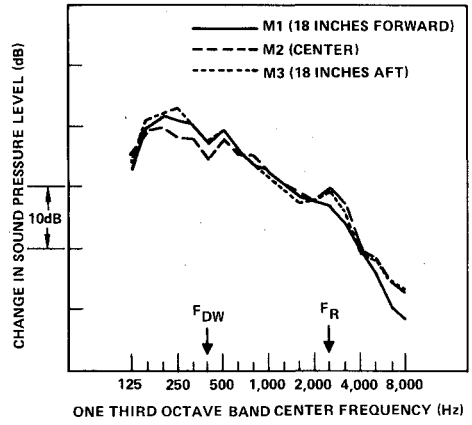

Fig. 4 Cylinder II interior noise spectra for a double-wall configuration.

microphones were used to represent the interior noise levels for noise reduction calculations. There were only minor differences between the three microphones as shown in Figs. 3 and 4. These results are typical of differences measured with other cylinder configurations.

Prediction Method

Theory

The prediction method used for this study is based on the theoretical developments of Smith[5] and Koval[6,7] for cylinder transmission loss and Beranek[8,9] for the inner wall incremental transmission loss. The Koval/Smith theory is suitable for analyzing axisymmetric cylinders at oblique angles of incidence with and without an external airflow. Originally derived for a free-field plane wave excitation, the theory is applicable to anechoic chamber tests at discrete angles of incidence. The mass and stiffness of stiffeners is smeared or averaged and then a monocoque analysis is performed. Development of the prediction method is continuing and Koval's treatment of cylinders with discrete stiffeners[10] is now being implemented.

Modification of Transmission Loss Theory for Treatment to Include an Air Gap Loss Factor

The discussion of the test data later in this paper will show that the agreement between theory and experiment for the unstiffened single-wall cylinder (cylinder I) as shown on Fig. 5 is very good; however, for the double-wall unstiffened cylinder, the unmodified theory underpredicts the experimental noise reduction (Fig. 6, "air gap loss factor" −0.0). By introducing an air gap loss factor of −2.0 in Fig. 6, one obtains satisfactory results. Before discussing comparisons with experimental data, a discussion of the theory is presented which provides a plausible physical rationale for the modification of the theory.

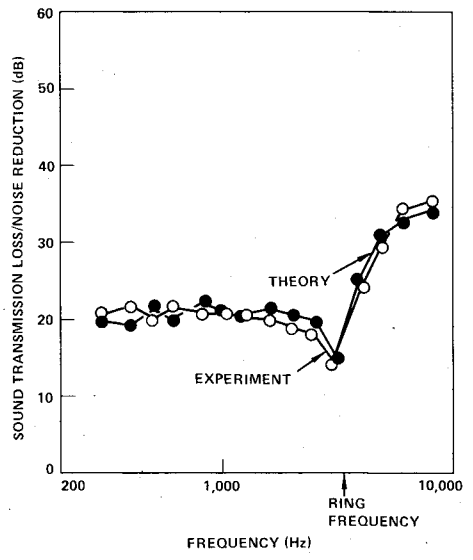

Fig. 5 Unstiffened cylinder: single wall, 20 in. diameter (cylinder I).

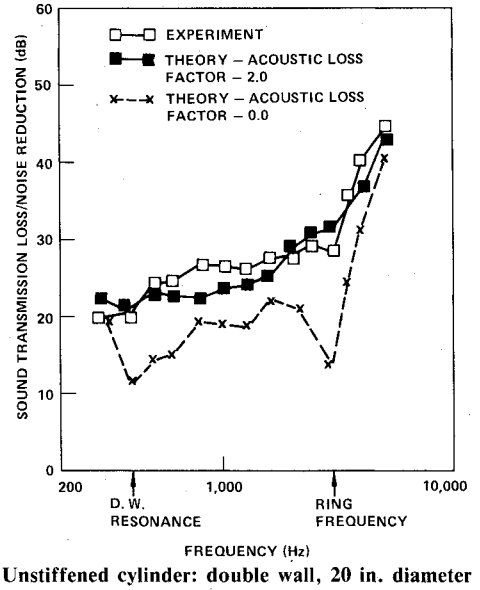

Fig. 6 Unstiffened cylinder: double wall, 20 in. diameter (cylinder II).

The theory for calculating transmission loss (TL) across air gaps and fiberglass blankets is based on Beranek's method.[8,9] For a given layer the incremental TL is

$$\Delta \mathrm{TL} = 20\log_{10} |P_I/P_T|$$

where P_I/P_T is the ratio of incident to transmitted sound pressure for the layer. From Ref. 8, the transmitted pressure ratio P_I/P_T is

$$P_I/P_T = \frac{\cosh[bd\cos\phi + \coth^{-1}(Z_2\cos\phi/Z_B)]}{\cosh[\coth^{-1}(Z_2\cos\phi/Z_B)]} \qquad (1)$$

where Z_B is the characteristic impedance of the transmitted layer and Z_2 is the termination impedance. The quantity b is the so-called propagation constant of the layer, having the dimensions of wave number (length^{-1}) and d is the layer thickness.

In the case of the present double-wall cylinders, the layer is an air gap terminated by a limp lead-vinyl-type cylindrical inner wall for which the stiffness has been assumed to be negligible; therefore, the termination impedance for the air gap is

$$Z_2 = j\omega m_2 + \rho_2 c_2 \qquad (2)$$

where the first term is the inner wall mechanical impedance according to mass law theory and the second term is the impedance of the air inside the cylinder. The characteristic impedance of the air gap is simply

$$Z_B = \rho_a c_a \qquad (3)$$

where ρ_a and c_a are the density and speed of sound within the air gap, respectively. For the present tests at sea-level laboratory conditions, $\rho_a = \rho_2$ and $c_a = c_2$; however, the subscripts are included to clarify the concepts.

The unique aspect of the present theory is the modification of the propagation constant b in such a manner to allow for energy dissipation in the air gap. Accordingly, the propagation constant is expressed as a complex number quantity

$$b = \omega/c_a(j + \eta_{ag}) \qquad (4)$$

The factor η_{ag} is herein called an air gap loss factor. Such a designation is appropriate for describing the decay of a plane wave propagating into a semi-infinite lossy medium such that

$$p(z) = p_0 \exp\{j\omega t - |b|z\} \qquad (5)$$

where z is the penetration distance into the lossy medium and p_0 is the pressure amplitude at $z = 0$.

The idea behind introducing such a factor was derived by analogy to Beranek's analysis[7] for fiberglass blankets and other porous media. A rigorous justification is not possible within the scope of this paper; however, some possible mechanisms by which energy is dissipated will now be considered in the following paragraphs.

Viscosity Effects (Mechanism 1)

Equation (1) is a result of one-dimensional wave propagation in the direction z, defined to be perpendicular to a pair of plane parallel walls which bound the air gap. The air gap is of finite length and is closed circumferentially; therefore, a more rigorous description of the forced acoustical motion within the annular cylindrical air gap must employ a standing wave description (in contrast to the traveling wave treatment of Refs. 1, 2, 8, and 9) which includes two kinds of Bessel functions to describe the radial modes, air gap acoustical modes of the type $\sin n\phi$ and $\cos n\phi$ to describe the circumferential motion, and sinusoidal modes to describe the axial standing waves. A redistribution of acoustical energy occurs, from radial modes into modes parallel to the walls. This process better facilitates energy dissipation via the effects of fluid viscosity of the air in the thin viscous boundary layers adjacent to the wall.

The Navier-Stokes equations of fluid motion when linearized for small acoustical motions fully describe the coupling process by which energy is transferred from acoustical modes perpendicular to the wall to acoustical modes parallel to the wall. The modes parallel to the wall are more efficient in their viscous dissipation via shearing action.

Vibration Mode Shape Mismatch (Mechanism 2)

Another source of a possible mechanism beyond the scope of the original theory of Refs. 1 and 2 is that the inner wall or trim panel vibration modes are likely to differ considerably from the outer wall or skin panel bay vibration modes. Typically, the trim panels are constructed with much larger dimensions. Trim panels are also generally very different from the outer wall in stiffness and mass characteristics. Furthermore, they are vented to the cabin pressure and hence are unpressurized. For the above reasons, the natural

vibration frequencies and mode shapes of the trim panels will, in general, be different from the outer wall panel modes. When an external sound field is applied, the outer wall will respond most strongly in the natural vibration modes of the outer wall panels. The trim panels, on the other hand, will respond most efficiently at their own natural frequencies and associated mode shapes which are, therefore, likely to be inefficiently coupled to the outer wall because of a dissimilarity of the responding vibration mode shapes when excited at a given frequency.

This second mechanism is not, in reality, one of dissipation, but has the same effect: reducing the amount of sound transmitted across the air gap.

Acoustically Slow Vibration Modes (Mechanism 3)

The response of the air gap cavity between the double walls is better described in terms of axial standing waves. As a model problem, a simplified flat double-wall analysis is given below. Let the sound pressure field expressed in the air gap be expressed as

$$p_I(x,y,z) = \sum_m \sum_n \{\sin k_m x \sin k_n y [A_{mn}\cosh(b_{mn}z) + B_{mn}\sinh(b_{mn}z)]\} e^{j\omega t} \quad (6)$$

where the propagation constant b carries double subscripts associated with the in-plane wave numbers, k_m and k_n

$$k_m = k_x = m\pi/L_x \qquad k_n = k_y = n\pi/L_y \quad (7)$$

which are associated with the dimensions L_x and L_y of the bounding panels. The wave equation inside the air gap requires that

$$\nabla^2 p_I + (\omega/c_a)^2 p_I = 0 \quad (8)$$

Therefore, Eqs. (7) and (8) require that the propagation constant be

$$b_{mn} = [(k_n^2 + k_m^2) - (\omega/c_a)^2]^{1/2} \quad (9)$$

Equations (6) and (9) have exactly the same form as for lossy porous media and for fiberglass blankets in the case where

$$(k_n^2 + k_m^2) - (\omega/c_a)^2 > 0 \quad (10)$$

This case will be designated as an "acoustically slow mode" for the air gap when bounded by two panels of length L_x and L_y. For an annular air gap bounded by concentric cylindrical shells, a similar argument prevails, but the radial motion must be described by appropriate Bessel functions.

The implication of this third mechanism is that large values of the "in-plane" wave numbers, k_m and k_n, cause a decay mechanism across the air gap [determined by Eqs. (6) and (9)] in a manner similar to a wave propagating in a lossy medium. The theory of Refs. 1, 2, and 5-7 is based on a traveling wave description of the axial motion, and these waves are all "acoustically fast."

In summary, the introduction of an "air gap loss factor" into the simplified traveling wave-type theory of Refs. 1 and 2 provides a convenient mechanism for predicting increased transmission loss for double-wall, sidewall acoustical treatments. The intent of this paper is to evaluate the required magnitude of the air gap loss factor using empirical transmission loss data for small, double-wall cylinders. The preceding analytical discussion has suggested several theoretical mechanisms for explaining why increased transmission loss may be expected in comparison to the original Beranek analysis which is restricted to oblique traveling wave transmission.[8,9]

Modification of Theory for Reverberant Field Environment

In defining the incident and absorbed power per unit of length for a cylinder in a free field, Smith[5] used the expressions,

$$\pi_i = P_0^2(2a)\cos\theta/(2\rho c) \qquad \pi_a = \tfrac{1}{2}\int_0^{2\pi} Re(p\dot{w}^*)a\,d\phi \quad (11)$$

where P_0 is the amplitude of incident pressure, a the radius of the cylinder, ρ the external air density, c the external speed of sound, p the acoustic pressure on the surface of the cylinder, $\dot{w}^*$ the radial velocity of the shell surface (complex conjugate), and ϕ the angular cylindrical coordinate.

In order to apply this theory to reverberant field excitations the incident power expression becomes

$$\pi_i = P_0^2(2\pi a)\cos\theta/(2\rho c) \quad (12)$$

With a plane wave in a free field the surface area per unit length that intercepts the incoming wave is simply $2a$, whereas in the reverberant field it is $2\pi a$. This accounts for the diffuse character of reverberant fields by assuming that the intensity of the incident acoustical field is constant over the entire circumference. Thus for the same exterior noise level as the free field, the input power is higher in the reverberant field. The theory assumes a fully absorbent interior space, and this condition was simulated for the laboratory tests described in this paper. Cylinder transmission loss is defined as

$$\text{TL} = 10\log\frac{\text{incident power}}{\text{absorbed power}}$$

An integration is performed over the incidence angle range from ± 87.5 deg to calculate the reverberant field transmission loss.

The relationship between noise reductions and transmission loss is[10]

$$\text{NR} = 10\log[1 + (\alpha S/\tau S)] \quad (13)$$

where

S = absorbing surface area
S_t = transmitting surface area
α = average absorption coefficient
τ = transmission coefficient
$S = S_t$
$\alpha \to 1.0$
$\tau \ll 1.0$
$\text{TL} = -10\log\tau$
$\text{NR} \cong \text{TL} + 10\log\alpha$

A total of six different configurations were tested, three single-wall and three double-wall as described in Table 1.

Theory vs Experiment

The 20 in. diameter unstiffened cylinder noise reductions are shown in Fig. 5. Single-wall or bare cylinder predictions match the experimental results extremely well over a broad frequency range of 300-6000 Hz. This would scale to a range of approximately 50-950 Hz for a narrow-body aircraft. Since there are no stiffeners on this cylinder the monocoque analysis is directly applicable, whereas with the stiffened cylinders the mass and stiffness of the stiffeners must first be averaged over the surface of the cylinder. When an inner wall or septum is added there is a significant difference between the experimental and theoretical results as shown in Fig. 6. In order to account for this difference two parameters were varied to bring the two results into agreement. First, the inner wall septum was assumed to be a low stiffness panel with variable damping loss factor. The assumption of structural damping loss factors as high as 1.0 for the inner wall had a negligible

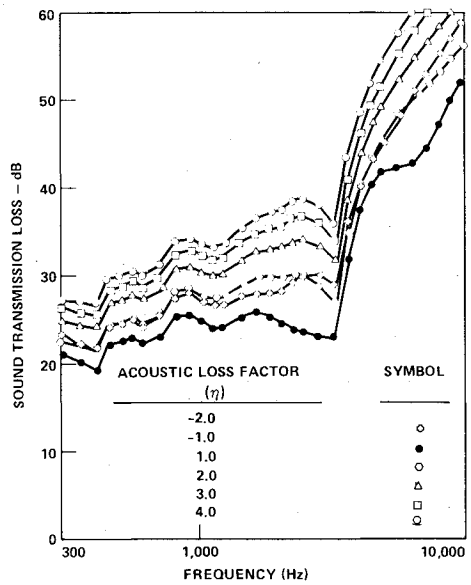

Fig. 7 Acoustic loss factor parametric study, 20 in. diameter unstiffened cylinder.

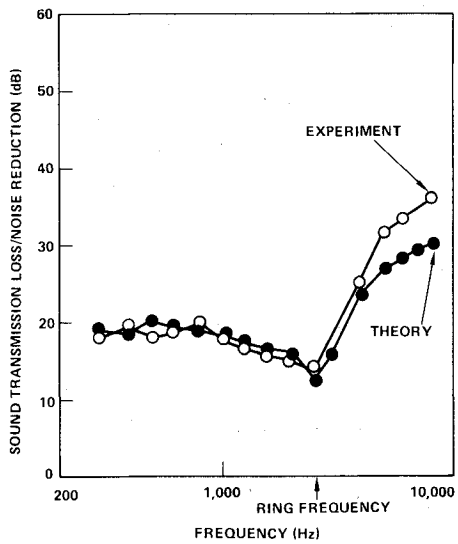

Fig. 8 Ring-stiffened cylinder: single wall, 24 in. diameter (cylinder II).

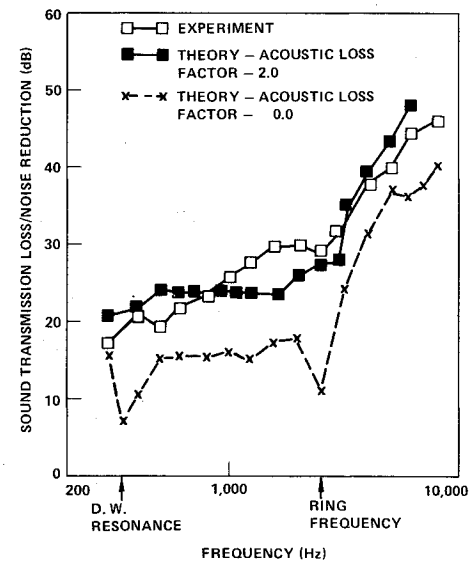

Fig. 9 Ring-stiffened cylinder: double wall, 24 in. diameter (cylinder II).

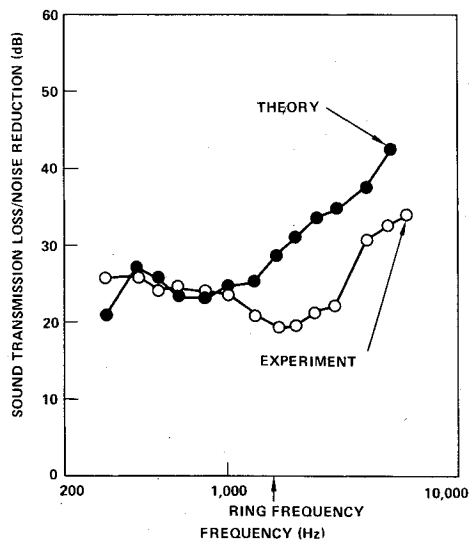

Fig. 10 Ring- and stringer-stiffened cylinder: single wall, 24 in. diameter (cylinder III).

effect on the calculated cylinder noise reduction. Since the predicted and experimental noise reductions were nearly identical for the single-wall cylinder and since the inner wall did not appear to be the source of the discrepancy, an air gap loss factor was introduced as discussed above.

The results of this study are shown in Fig. 7 and a value of -2.0 provided the closest agreement between theory and experiment.

Cylinder II is a ring-stiffened cylinder for which the incremental mass and stiffness provided by the widely spaced stiffeners is considered modest. Comparisons between theory and experiment are shown in Fig. 8. The single-wall results show good agreement up to nearly two times the ring frequency. The first breathing mode of the cylinder is referred to as the ring frequency. Estimates of the ring frequency can be determined from

$$f_R = C_L/2\pi R$$

where C_L is the longitudinal elastic propagation speed wave in the cylinder and R the radius of cylinders.

In view of the very close agreement between theory and experiment shown for the unstiffened cylinder, the differences shown for this cylinder are attributed to averaging or smearing of the stiffener properties in the analysis.

Double-wall configuration results, presented in Fig. 9, are not nearly as close as the single-wall comparisons. Both the inner wall damping loss factor and the airspace acoustic loss factor were varied and the predicted cylinder noise reductions were compared to the experimental results. Increasing the damping loss factor of the inner wall had a negligible effect on the results. When the acoustic loss factor for the airspace between the walls was varied, once again the value of -2.0 for the attenuation constant provided the closest agreement between theory and experiment. As shown in Figs. 8 and 9 the agreement between theory and experiment for both the single- and double-wall configurations is good but not as close as that obtained for the unstiffened cylinder.

Cylinder III is stiffened with both rings and stringers spaced at 8.25 and 4.0 in., respectively. This represents a significant increase in stiffness relative to the unstiffened cylinder which had the same skin thickness and a slightly smaller diameter. As shown in Fig. 10 the agreement between theory and experiment is quite good up to 1000 Hz for the

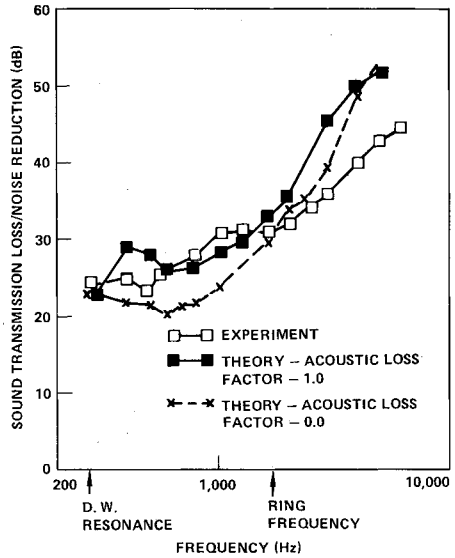

Fig. 11 Ring- and stringer-stiffened cylinder: double wall, 24 in. diameter (cylinder III).

single-wall configuration. However, at frequencies above 1000 Hz there are differences in excess of 10 dB.

When the results for the single wall configurations of all three cylinders are reviewed the following observations can be made:

1) Theoretical and experiment results are in close agreement at frequencies below 1000 Hz.

2) At frequencies greater than 1000 Hz the differences between theory and experiment are a function of the amount of stiffening.

These results are thought to be caused by the averaged stiffener monocoque analysis that is used. Koval[10] has recently extended the theory to treating the stiffeners as discrete rather than averaged elements. Modification of the Lockheed prediction method is in progress to incorporate the discrete stiffener analysis. Additional studies will be initiated utilizing the discrete stiffener analysis when it is available.

Double-wall noise reduction results for cylinder III are shown in Fig. 11. Parametric studies of inner wall damping loss factor and between wall airspace acoustic loss factor were again performed. Once again the inner wall structural damping loss factor changes had a negligible effect on configuration noise reduction. However, the best match between theory and experiment was obtained with an air gap acoustic loss factor of -1.0 instead of -2.0 as was obtained with the other two cylinders. The acoustic loss factor is effective in minimizing the effects of the mass-spring-mass double-wall resonance and the characteristic loss of attenuation in the vicinity of the ring frequency. Double-wall resonance frequency can be calculated from

$$F_{DW} = 170 \Big/ \left[\left(\frac{M_1 M_2}{M_1 + M_2} \right) d \right]^{1/2}$$

where M_1 and M_2 are the surface densities of the outer and inner walls in pounds per square foot and d is the air gap width expressed in inches.

An acoustic loss factor will probably still be required even with an improved analytical model which treats stiffeners as discrete elements. This is demonstrated by the unstiffened cylinder analysis which is not compromised by the averaging of stiffener properties and showed good agreement between theory and experiment for the single-wall cylinder. Use of the acoustic loss factor suggests that the double-wall mass-spring-mass resonance is either not occurring or it is a very weak resonance. It also suggests that the acoustic coupling between the inner and outer walls is a function of outer wall stiffness. This can be observed in Figs. 6, 9, and 11 for the double-wall results. The unstiffened and lightly stiffened cylinders showed much greater differences between theory and experiment, except at the higher frequencies.

Conclusions

Full-scale aircraft noise reduction data are desirable but extremely expensive to obtain; therefore, small-scale cylinder tests represent a cost effective alternative, if properly interpreted. When performing small-scale cylinder tests in lieu of full-scale aircraft tests, it is important to recognize that the models are axisymmetric idealized fuselage structures. To the extent that they simulate real aircraft fuselage structural responses, the agreement between theory and experiment is encouraging. However, the simulation of aircraft structures must be more realistic analytically as well as experimentally in order to develop reliable prediction methods.

The present paper has presented what is believed to be the first published experimental data on the noise reduction of double-wall cylinders. The data are regarded as being of considerable importance as a means of evaluating the accuracy of analytical predictions, since double-wall cylindrical configurations are representative of a highly mass efficient noise reduction treatment design intended for high-speed turboprop or propfan designs. The efficiency of double-wall designs is pertinent to propfan-powered aircraft which are characterized by much higher blade passage frequencies than conventional propellers. The experimental data are shown to be in reasonable agreement with analytical predictions of the authors, subject to several qualifications already discussed herein. The small-scale tests discussed here are one of the precursors to some large-scale fuselage tests conducted under a recent NASA Langley study which will be published soon.[4]

References

[1] Revell, J.D., Balena, F.J., and Koval, L.R., "Analytical Study of Interior Noise Control by Fuselage Design Techniques on High-Speed, Propeller-Driven Aircraft," NASA CR 159222, April 1980; also *Journal of Aircraft,* Vol. 19, Jan. 1982, pp. 39-45.

[2] Revell, J.D., Balena, F.J., and Koval, L.R., "Analysis of Interior Noise Control Treatments for High-Speed Propeller-Driven Aircraft," *Journal of Aircraft,* Vol. 19, Jan. 1982, pp. 31-38.

[3] Rennison, D.C., Wilby, J.F., Marsh, A.H., and Wilby, E.G., "Interior Noise Control Prediction Study for High-Speed Propeller-Driven Aircraft," NASA CR 195200, Sept. 1979.

[4] Prydz, R.A., Revell, J.D., Hayward, J.L., and Balena, F.J., "Evaluation of Advanced Fuselage Design Concepts for Interior Noise Control on High-Speed Propeller-Driven Aircraft," NASA CR 165960, Sept. 1982.

[5] Smith, P.W. Jr., "Sound Transmission Through Thin Cylindrical Shells," *Journal of the Acoustical Society of America,* Vol. 29, No. 6, June 1957, pp. 721-729.

[6] Koval, L.R., "On Sound Transmission into a Thin Cylindrical Shell Under Flight Conditions," *Journal of Sound and Vibration,* Vol. 48, No. 2, pp. 265-275.

[7] Koval, L.R., "On Sound Transmission into a Stiffened Cylindrical Shell Under Flight Conditions," AIAA Paper 76-549, July 1976.

[8] Beranek, L.L., "Acoustical Properties of Homogeneous Isotropic Rigid Tiles and Flexible Blankets," *Journal of the Acoustical Society of America,* Vol. 19, No. 4, July 1947, pp. 556-568.

[9] Beranek, L.L., "Sound Transmission Through Multiple Structures Containing Flexible Blankets," *Journal of the Acoustical Society of America,* Vol. 21, No. 4, July 1949, pp. 419-428.

[10] Koval, L.R., "On Sound Transmission into a Stiffened Cylindrical Shell With Rings and Stringers Treated as Discrete Elements," *Journal of Sound and Vibration,* Vol. 71, No. 4, 1980, pp. 511-521.